

Available online at www.sciencedirect.com**ScienceDirect**

Physics Procedia 65 (2015) 278 – 281

Physics

Procedia

27th International Symposium on Superconductivity, ISS 2014

Stress Analysis and Bobbin Structure Optimization Design of a 35kV HTS-Controllable Reactor

Z. Wang *, L. Ren, S. Shen, M. Song, Y. Zhang, H. Liu, L. Chen, B. Yu, N. Hu

State Key Lab of Advanced Electromagnetic Engineering and Technology (R&D Center of Applied Superconductivity, Huazhong University of Science and Technology), 1037 Luoyu Road, Wuhan, 430074, P. R. China

Abstract

A 35kV high temperature superconducting controllable reactor (HTS-CR) is under development and the electromagnetic design has been completed. Due to the AC conditions, the thermal stress caused by AC losses can be so strong that the stress analysis should be carried out to verify that the maximum stress under different operating conditions is in appropriate range. In addition, Lorentz force of HTS windings will impact the bobbin structure of the HTS windings which will endanger the 35kV HTS-CR. Stress analysis is important for the design of a mechanically stable structure. This paper provides the analysis of the bobbin structure and its result of optimization design considering the requirements of safety and cooling.

© 2015 The Authors. Published by Elsevier B.V. This is an open access article under the CC BY-NC-ND license (<http://creativecommons.org/licenses/by-nc-nd/4.0/>).

Peer-review under responsibility of the ISS 2014 Program Committee

Keywords: thermal stress analysis; bobbin structure; optimization design

1. Introduction

With the development of high-temperature superconducting wires, their application fields has expanded further into industrial magnets. A 35kV HTS-CR is under development in China and the electromagnetic design has been completed. This paper analyzes the thermal stress, electromagnetic stress of HTS coil and bobbin structure through the FEM method. Detailed analysis has been carried out on the internal stress in the double pancake coil (DPC), the maximum stress and stability of the bobbin structure. In order to optimize the structure, consideration has to be taken into three variables, the thickness of the bobbin T , the angle ratio of slot α and the number of rod N . In the end, the article presents the optimized results of the skeletal structure.

2. Structure and operating conditions of the HTS-CR

2.1. Basic parameters of 35kV HTS-CR

A 35 kV/3.5MVA HTS-CR mainly contains of a core, main winding and two HTS windings. The main winding is made of copper wires, and is connected to the 35 kV electrical power system. A prototype of HTS-CR has been developed in our previous work. The 35 kV/3.5MVA HTS-CR has the same working principle as the HTS-CR

* Corresponding author. Tel.: +86-27-8754-4755; fax: +86-27-8754-0937.
E-mail address: hustwzs@live.com

prototype, which is described in detail in reference [1]. When both windings of HTS-1 and HTS-2 are open-circuit, the main magnetic flux passes through the middle core column and the current of main winding is $50\pm 2A$. When only HTS-1 is short-circuit, the induced current of HTS-1 is $135.8A$, the space between HTS-1 and main winding provides the channel and the current of main winding reaches $75\pm 2A$. While only HTS-2 is short-circuit, the induced current of HTS-2 is $139.9A$, the space between HTS-2 and main winding provides the channel and the current of main winding becomes $100\pm 2A$. Fig.1 (a) is the schematic diagram of the 35kV HTS-CR. The non-magnetic material epoxy and G10 were used as the support structure in order to reduce losses. Fig.1 (b) is the original bobbin structure of the HTS windings designed based on the electromagnetic parameters. The gap between every two pancakes is set to 7 or 12mm. SCS40100CF YBCO tapes produced by SuperPower are used and the total length of the tapes is fixed and equal to 10 km. The mechanical and thermal properties of selected materials are shown in Table 1.

Table 1. Mechanical and thermal properties of the selected materials at 65–80K.

Material	Young's modulus E (Gpa)	Poisson's ratio ν	Shear modulus G (Gpa)	Thermal Conductivity (W/m·k)	Thermal Expansion (1/K, refers $T=293K$)	Heat Capacity (J/kg·K)
Ni-W	205	0.33	76.8	174	$2.17e-6$	139.2
Copper	100	0.31	38.17	550	$3.0e-6$	173
Silver	90	0.37	32.8	500	$3.6e-6$	166.2
Kapton	2.45	0.38	0.88	0.2	$2.0e-5$	587.7
Epoxy	28	0.28	10.94	0.2	$4.78e-5$	511.3
G-10	36	0.33	13.53	0.35	$9.9e-6$	500.5

As the HTS tape is a multi-layered structure, the mechanical properties of the HTS tape can be calculated by the multi-layered materials principle based on Table 1. Thus the HTS tape equals an orthotropic material. It's wise to treat the HTS tapes as a unit when analyzing the stress of the coil skeleton.

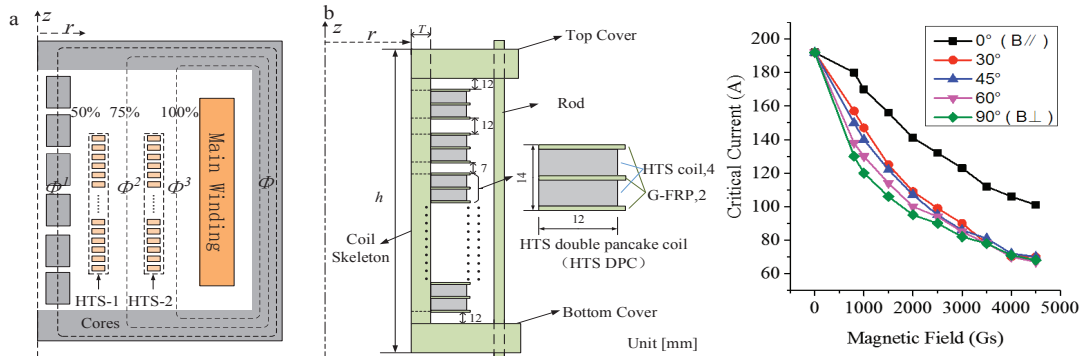


Fig. 1. (a) Schematic diagram of the 35kV HTS-CR; (b) Structure of the HTS winding; Fig.2 Critical current under different magnetic field

2.2. Operation conditions of the magnet

The 35kV HTS-CR is designed to work under AC condition with the frequency of 50Hz. The significant feature is that the magnetic flux leakage is relatively large in order to obtain higher reactance value. This characteristic leads to great AC losses which are the main sources of the thermal stress. The AC losses of the HTS coils are calculated by equation (1).

$$\frac{\partial(\mu_r \mu_0 \vec{H})}{\partial t} + \rho_{sc} \nabla \times \vec{J} = 0 \quad \text{where} \quad \vec{J} = \nabla \times \vec{H} \quad \text{and} \quad \rho_{sc} = \frac{E_c}{J_{cB}} \left| \frac{J}{J_{cB}} \right|^{n-1} \quad (1)$$

In formula (1) μ_0 , μ_r and ρ_{sc} are the vacuum magnetic permeability, relative magnetic permeability and resistivity, respectively. For a superconductor, ρ_{sc} depends on the current density and can be represented by a nonlinear power-law relation derived from measured current–voltage characteristics. We have tested the critical current of the tape under different angle of magnetic fields and got a curve of $J_c(B, \theta)$ through the method in reference [2]. Fig.2 is the critical current under different fields. The AC Losses are calculated by using the method in reference [2] too.

Fig.3 is the average magnetic field distribution on some DPCs of HTS windings. Obviously, perpendicular field is relatively high at both ends of the shorting HTS winding. This feature leads to the great losses at both ends of the HTS winding. Comparing Fig.3 (a) and (b) we can find that when HTS-2 is short-circuit, the average magnetic field on HTS-2 is high than that on HTS-1 when HTS-1 is short-circuit. Fig.4 shows the calculation result of AC losses on

some double pancake coils. The number sequence is from top to bottom. Apparently, both electromagnetic and thermal stress will concentrated on end DPCs. Therefore, the following analysis focuses on the top end DPC of HTS-2.

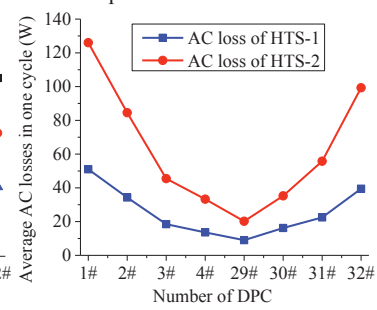
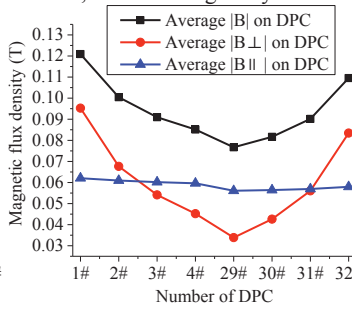
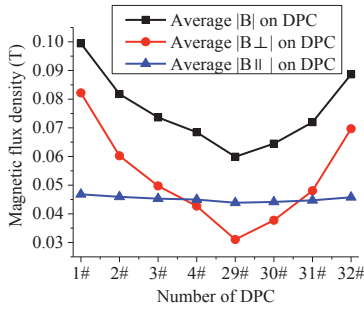


Fig. 3. (a) Magnetic field on DPCs of HTS-1; (b) Magnetic field on DPCs of HTS-2. Fig. 4 Losses Distribution of HTS coils;

3. Stress analysis and bobbin structure design

3.1. Thermal and electromagnetic stress analysis

The dominant stress patterns of a solenoid-type magnet are circumferential tension or hoop stress and axial compression. The transient stress has been analyzed based on the FEM. Through the above analysis, the maximum losses at the top double pancake of the HTS-2 where the thermal stress will reach maximum.

The theory of stress analysis has been classically defined in previous works [3]. The electrometric stress analysis is described by equation (2) and equation (3) is the thermal stress formulas.

$$r \frac{\partial \sigma_r}{\partial r} + \sigma_r - \sigma_\theta + r \cdot J(r) \cdot B(r) = 0 \tag{2}$$

Where r is the radius from the origin, σ_r is the radial stress, σ_θ is the hoop stress, J is the current density, and B is the magnetic field. The governing equation requires numerical expansion, which is well defined elsewhere [3].

$$\begin{aligned} \frac{\partial \sigma_r}{\partial r} + \frac{\partial \tau_{rz}}{\partial z} + \frac{\sigma_r - \sigma_\theta}{r} + f_r &= 0 & \sigma_r &= 2G \left[\frac{1-\nu}{1-2\nu} \frac{\partial v}{\partial r} + \frac{\nu}{1-2\nu} \left(\frac{u}{r} + \frac{\partial \omega}{\partial z} \right) \right] - \beta T \\ \frac{\partial \sigma_z}{\partial z} + \frac{\partial \tau_{rz}}{\partial r} + \frac{\tau_{rz}}{r} + f_z &= 0 & \sigma_\theta &= 2G \left[\frac{1-\nu}{1-2\nu} \frac{\nu}{r} + \frac{\nu}{1-2\nu} \left(\frac{\partial u}{\partial r} + \frac{\partial \omega}{\partial z} \right) \right] - \beta T \\ \tau_{rz} &= G \left(\frac{\partial \omega}{\partial r} + \frac{\partial u}{\partial z} \right) & \sigma_z &= 2G \left[\frac{1-\nu}{1-2\nu} \frac{\partial \omega}{\partial z} + \frac{\mu}{1-2\nu} \left(\frac{\partial u}{\partial r} + \frac{u}{r} \right) \right] - \beta T \end{aligned} \tag{3}$$

In equation (3) r_z is the axial stress, f_r is the radial volume force, and f_z is the axial volume force. The volume force comes from deformation of materials under different temperatures. u is the displacement, ω is the axial displacement, β is coefficient of thermal stress, G is the Shear modulus, and ν is the Poisson's ratio.

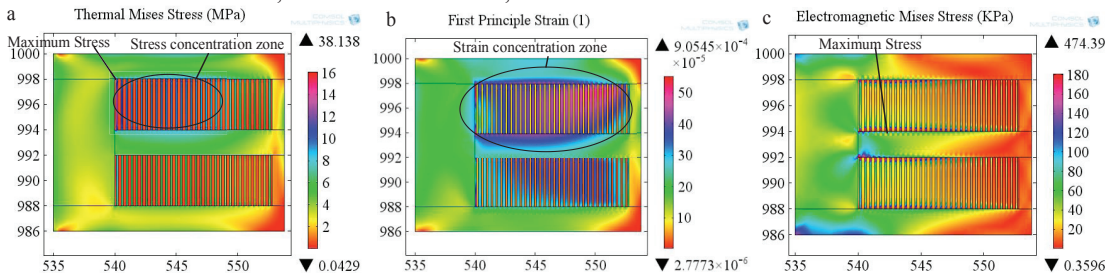


Fig. 5. (a) Thermal stress distribution; (b) Thermal strain distribution; (c) Electromagnetic stress distribution;

In the analysis of the thermal stress, the boundary temperature distribution of the DPC is obtained from the result of thermal analysis. We have designed a closed cycle cooling system for the HTS-CR and the thermal analysis has been finished. More details shall be introduced in the future work. A magnetic-mechanical coupling analysis was used to calculate the electromagnetic stress of the DPC.

To clarify, the parallel winding of the multiple tapes makes the pretension during processing so difficult to be precisely controlled that the effect from the cool of room temperature to the thermal contraction at work is not considered temporarily. More detailed analysis will be carried out after decision of the processing scheme. In analysis the strain reference temperature is set to 65K. Fig.5 is the stress and strain distribution on top DPC of HTS-2. The maximum thermal stress caused by AC losses is $38.138\text{MPa} \ll 150\text{MPa}$ (the yield stress of HTS tape). The maximum electromagnetic stress is 474.39KPa , nearly to be neglected compared to thermal stress. This distribution of stress will provide a great assistance to get a better pretension design. The thickness of epoxy plate on both sides of HTS pancake is 2 mm (Fig. 1 (b)) in order to guarantee the insulation level.

3.2. Optimization of bobbin structure

In order to reduce AC losses and the internal thermal stress of DPCs, the power of magnetic field must be weakened. After analysis, however, that will result in a great increase of HTS tapes and total cost to be hard to afford. Moreover, the internal Dewar cooling space can hardly be enlarged and thus enough LN_2 in Dewar has to be guaranteed through the optimization of skeleton structure. So we slot the frame to facilitate the flow of LN_2 . However, the size and distribution of the slots will impact the stress of the structure, which should be optimized to get the best solution. The constraint condition is that the maximum stress is less than 70% the yield stress (100MPa). The thickness of the bobbin T , the angle ratio of slot α and the number of rod N are the variables to be optimized.

Fig.6 (a) is the flowchart of the optimization algorithm. A thermal-structural coupling analysis was used for the total stress analysis of bobbin structure. AC losses are the heat load, boundary temperature came from thermal analysis, and both radial and axial components of total electromagnetic force on each HTS DPC were fitting to curves as the force load. The conjugate heat transfer module was used for the cooling effect of the LN_2 . In the optimization of bobbin structure, we set the strain reference of temperature to 293K. That means the main reason for the stress may be the thermal stress caused by the cooling process from room temperature to the cryogenic temperature.

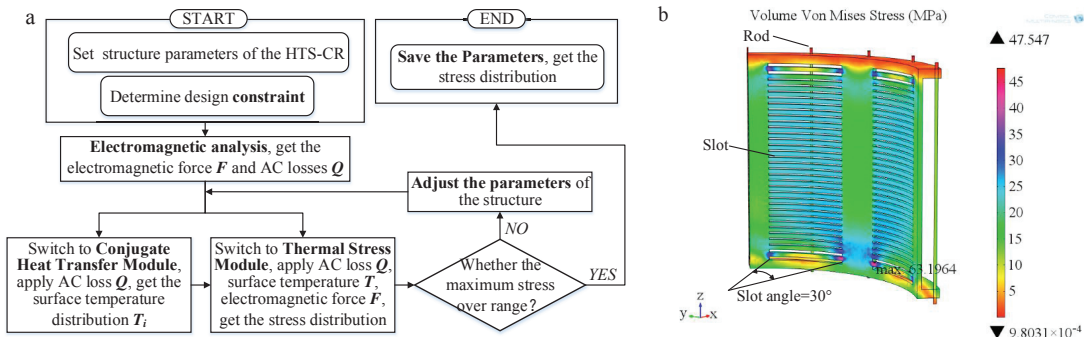


Fig. 6. (a) The flowchart of optimization algorithm; (b) The stress distribution of optimized structure

The objective is to find optimal parameters that the structure is most stable. For convenience of processing, the range of slot angle is defined as $[30^\circ \text{ per } 45^\circ, 45^\circ \text{ per } 60^\circ, 60^\circ \text{ per } 90^\circ, 75^\circ \text{ per } 90^\circ]$ and the range of rod number is $[4, 6, 8, 12, 16, 24]$. The thickness of the bobbin is between 10 mm and 30 mm. Ultimately, the thickness of the bobbin is calculated as 20mm, the number of rod is 16 and the slot angle is 30° per 45° . Fig.6 (b) is the stress distribution (1/4 model) of optimized structure and the maximum stress of the bobbin is 63.19MPa. Due to the great AC losses at both ends of the HTS winding, the slot at the ends suffer the maximum stress. However, stress of most regions is far smaller than the maximum which proves the stability of the structure.

4. Conclusion

In this paper, the basic parameters and operating conditions of 35kV HTS-CR have been given. Based on these parameters, thermal and electromagnetic stress of both HTS coil and bobbin structure has been analyzed. In the end, an optimal bobbin structure has been given out. According to the design results, the magnet will be fabricated and tested. More details shall be introduced in the future work.

References

- [1] Tang Y, Ren L, Song M, et al. Development of A Leakage Flux-Controlled Reactor[J]. 2014.
- [2] Zhang M, Kvitkovic J, Pamidi S V, et al. Experimental and numerical study of a YBCO pancake coil with a magnetic substrate[J]. Superconductor Science and Technology, 2012, 25(12): 125020.
- [3] Gray W H, Ballou J K. Electromechanical stress analysis of transversely isotropic solenoids[R]. Oak Ridge National Lab., TN (USA), 1977.